Int. J. Solids Structures Vol. 15, pp. 251–260

0020-7683/79/0301-0251/$02.00/0

AN OPTICAL METHOD OF GENERATING SLOPE AND CURVATURE CONTOURS OF BENT PLATES

F. P. CHIANG† and T. Y. KAO‡

Department of Mechanical Engineering, College of Engineering and Applied Science, State University of New York, Stony Brook, NY 11794, U.S.A.

(*Received* 31 *March* 1978; *in revised form* 17 *July* 1978)

Abstract—In order to determine the state of stress of a thin plate under transverse elastic bending, it is necessary to have the curvature value at each and every point of the bent plate. Most experimental methods yield deflection as the primary data which have to be differentiated twice for the stress calculations. Since numerical differentiation is an inherently inaccurate process, it should be avoided if at all possible. In this paper a method is devised whereby either the first derivative (slope) or the second derivative (curvature) of the plate deflection is obtained directly in the form of slope or curvature contour fringes, thus reducing or eliminating the necessity of numerical differentiation. Examples to both static and dynamic problems are presented.

INTRODUCTION

Experimental full-field methods of solving plate bending problems may be classified into two categories: one that measures the interior stress (or its analog) directly, and one that measures (either directly or indirectly) the surface deformation. Examples of the first type are the photoelastic methods such as that of Goodier *et al.*[1] and Drucker[2]. Techniques of the second group may be further divided into three types: those that measure deflection[3–12], slope[13–22] and curvature[23–26], respectively, of the deformed plate. Among the methods of deflection measurement, the simplest is perhaps the shadow Moiré method[3–7]. Among the many slope measuring techniques the most popular and widely used is the Ligtenberg reflection Moiré method[13] and its derivatives[14–17]. Methods that yield curvature directly are limited in number, and all but one employ the superposition technique to give curvature contours. The one by Chiang and Bailangadi[26] uses a method of optical spatial filtering.

From the point of view of error involved, a curvature measurement method is preferred over a slope measurement method, and which in turn is preferred over a deflection measurement method. This is so because of the ever present and oftentimes large errors associated with numerical differentiation of experimental data. In this paper we offer an optical method which can yield either slope or curvature contours *directly*, thereby eliminating partially or totally the differentiation error. It should perhaps be emphasized that with the proposed method the curvature contours are obtained without either double exposure, superposition or optical processing. As a result the method can be directly applied to wave propagation problems.

Basically the method employs a relatively coarse grating to obstruct a beam of light that is reflected from a mirrored surface of a plate model. In a way it is similar to the methods of Ronchi who uses gratings to test mirrors and lenses and who has summarized these methods in a recent article[27]. However the methods presented here are different and mainly for the purpose of studying thin plates under transverse bending.

THEORY OF SLOPE CONTOURING

The optical arrangement of the method is as shown in Fig. 1. The mirrored surface of a plate model p is illuminated by a *beam* of parallel light with angle α_x from the normal in the x–z plane. (The inclination of the beam in the y–z plane is immaterial so long as it is small.) The reflected light rays are collected by a field lens L and form the image of the model plate at plane I. At the focal plane of the field lens, an amplitude grating of pitch P is installed with its lines normal to the x-axis. Before subject to transverse bending the plate is assumed to be flat. Thus all the reflected light rays are converged into a point (lens aberration is assumed to be negligible). Thus the image field is either dark or bright or somewhere in between depending

†Professor of Engineering.
‡Post-doctoral Fellow.

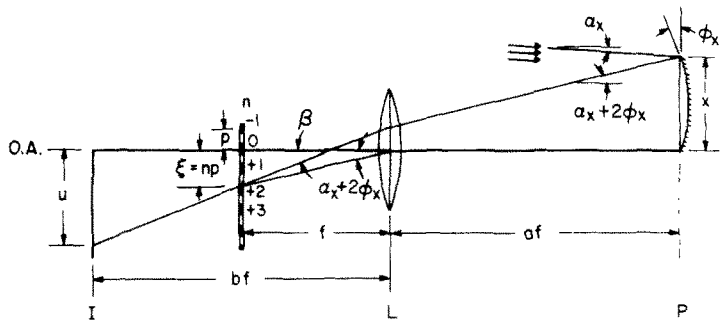

Fig. 1. Optical arrangement of the method.

upon where on the grating the light is focused. After deformation of the plate the light rays will no longer concentrate into a point. Rather they will be spread out casting shadows of the grating lines on the image plane. And it will be shown that these shadows (hereafter referred to as the shadowgram) are contour fringes of slope of the deformed (bent) plate along the direction normal to the grating lines.

As shown in Fig. 1, the object and image distances are denoted by af and bf, respectively, where f is the focal length of the field lens. A ray that impinges upon the mirrored plate surface with angle α_x will be returned with an angle $\alpha_x + 2\phi_x$ where ϕ_x is the local slope along the x-axis of the deflected plate. The deflection is assumed to be small such that the spatial position of a point before and after deformation may be assumed stationary. The reflected ray is further bent by the field lens into angle β, intersecting the grating at a distance ξ, and reaching the image plane at distance u, both measured from the optical axis of the system. It is seen from the figure that $\xi = f \tan(\alpha_x + 2\phi_x)$. Denoting $\xi_0 = \xi$ when $\phi_x = 0$, one has $\xi_0 = f \tan \alpha_x$. The distance scanned by the light ray due to the presence of ϕ_x is then

$$\Delta\xi = \xi - \xi_0 = f \tan(\alpha_x + 2\phi_x) - f \tan \alpha_x = f \frac{\tan 2\phi_x \sec^2 \alpha_x}{1 - \tan \alpha_x \tan 2\phi_x}. \quad 1)$$

If $2\phi_x$ is small and $\tan \alpha_x$ is of order one or less, eqn (1) may be approximated by

$$\Delta\xi = \frac{2f\phi_x}{\cos^2 \alpha_x} \quad \text{or} \quad \phi_x = \frac{\Delta\xi \cos^2 \alpha_x}{2f}. \quad 2)$$

Denoting n as the parameter of individual grating lines as shown, with zero coinciding with ıe optical axis and positive numbers downward; and with $\partial w/\partial x = \phi_x$, one has

$$\frac{\partial w}{\partial x} = \frac{(n - n_0)p}{2f} \cos^2 \alpha_x \quad \text{or} \quad \frac{\partial w}{\partial x} = \frac{Np \cos^2 \alpha_x}{2f} \quad 3)$$

where N is the fringe order, and p pitch of the grating. It is seen that the fringes (i.e. ıe shadow of the grating lines) are contours of slope.

The grating used for slope contouring should be fairly coarse. In most experime ts performed in this study the grating density was about 4 lpcm.

THEORY OF CURVATURE CONTOURING

The optical arrangement for contouring curvature is identical to that for slope co.. ıg except that finer grating is used. The grating should be fine enough that the effect of ht diffraction is observable at the image plane. As schematically shown in Fig. 2 when a beam of light passes through a fine grating it is diffracted into many beams (diffraction orders) and the angle of deviation between any two neighboring orders is given by $\theta = \lambda/p \cos \beta$, where λ is the wavelength. The result of diffraction is that there are multiple images at the image plane with a relative shift between two neighboring images given by

$$\Delta u = z \tan(\beta + \theta) - \tan \beta = z \frac{\sec^2 \beta \tan \theta}{1 - \tan \beta \tan \theta}. \quad (4)$$

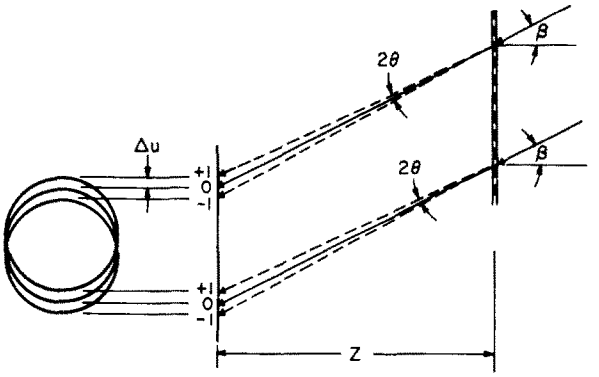

Fig. 2. Image shifting due to diffraction.

For moderately fine gratings (line density in the range of 2–4 lpmm) the diffraction angle is quite small; one may assume that $\tan\theta \sim \theta$. Furthermore if $\tan\beta$ is of order one or less, eqn (4) can be simplified into

$$\Delta u = \frac{\lambda z}{p\cos^3\beta}. \tag{5}$$

If the grating used is such that it only has two equal intensity first order diffractions, one may express the intensity variation of the 0 and ± 1 order images of the grating as

$$I_0(u) = \frac{1}{2}[1 + \cos 2n(u)\pi], \tag{6}$$

$$I_1(u) = \frac{1}{2}\gamma_1[1 + \cos 2n(u + \Delta u)\pi], \tag{7}$$

$$I_{-1}(u) = \frac{1}{2}\gamma_1[1 + \cos 2n(u - \Delta u)\pi], \tag{8}$$

where $\gamma_1 = I_1/I_0 = I_{-1}/I_0$, and n the grating line parameter as before. Since all these three shadowgrams are superimposed together, the total intensity is given by the sum, i.e.

$$I_T(u) = \frac{1}{2}\{1 + 2\gamma_1 + \cos 2n\pi + \gamma_1[\cos 2(n + \Delta n)\pi + \cos 2(n - \Delta n)\pi]\}$$

$$= \frac{1}{2}\{1 + 2\gamma_1 + \cos 2n\pi[1 + 2\gamma_1 \cos 2(\Delta n)\pi]\}. \tag{9}$$

In the above equation the following substitution has been made: $n(u \pm \Delta u) = n \pm \Delta n$, where $\Delta n \sim (\Delta u)(\partial n/\partial u)$. This equation depicts essentially the pattern of the zero order shadowgram of slope fringes modulated by another sinusoidal enveloping fringe of period Δn. For simplicity it shall be assumed that $\gamma_1 = 1/2$. (This is made so as to bring out the physics of the method. γ_1 of different values are treated in a report[31]; and it is shown that the basic conclusion is not altered except the visibility of the curvature fringes.) Thus one has

$$I_T(u) = \frac{1}{2}\{2 + \cos 2n\pi[1 + \cos 2(\Delta n)\pi]\}. \tag{10}$$

For $\Delta n = 0, \pm 1, \pm 2, \ldots$, eqn (10) reduces to

$$I_T(u) = 1 + \cos 2n\pi \tag{11}$$

which is nothing but the zeroth order shadowgram of the slope fringe with twice the intensity. But for $\Delta n = 1/2, 3/2, 5/2, \ldots$, eqn (10) reduces to $I_T(u) = 1$, which means that the slope fringe has disappeared. In between, the basic pattern of eqn (11) still prevails but with reduced

visibility. Thus the enveloping fringes manifest themselves in terms of the visibility of the original slope fringes, ranging from one as given by eqn (11) to zero given by $I_T(u) = 1$. Actually these enveloping fringes are essentially Moiré fringes resulted from the superposition of all orders of the shadowgram of slope fringes.

The meaning of these enveloping fringes may be interpreted as follows. They represent the difference of slope fringe values (as given by Δn) over a shifted distance Δu. Thus from eqns (3) and (5) one has

$$\frac{\Delta\phi_x}{\Delta u} = \frac{\phi_x(u+\Delta u) - \phi_x(u)}{\Delta u} = \frac{n(u+\Delta u) - n(u)}{\Delta u}\frac{p\cos^2\alpha_x}{2f}$$
$$= \frac{\Delta n p^2 \cos^2\alpha_x \cos^3\beta}{2fz\lambda}. \tag{12}$$

Noting that $z = (b-1)f$, and the magnification of the system being $M = u/x = b/a = (b-1)$ one has

$$\frac{\partial^2 w}{\partial x^2} \cong \frac{\Delta\phi_x}{\Delta x} = (b-1)\frac{\Delta\phi_x}{\Delta u}, \tag{13}$$

and eqn (12) is reduced to

$$\frac{\partial^2 w}{\partial x^2} = \frac{N' p^2 \cos^2\alpha_x \cos^3\beta}{2\lambda f^2}, \tag{14}$$

where $N' \equiv \Delta n$ is the new order of the enveloping fringes. If the field lens has a long focal length and small aperture (i.e. small f/number) the angle β may be approximated by α_x. Thus eqn (14) is further simplified to

$$\frac{\partial^2 w}{\partial x^2} \cong \frac{N' p^2 \cos^5\alpha_x}{2\lambda f^2}. \tag{15}$$

One has then the enveloping (Moiré) fringes as contours of curvature.

In order to obtain the stress information one needs, of course, the curvature values along two perpendicular directions and the twist. For the fringe pattern to represent the curvature along y-direction one simply turns the grating 90°; the field equation is identical to eqn (15) with $\partial^2 w/\partial y^2$ replacing $\partial^2 w/\partial x^2$.

The twist may be calculated by obtaining a third curvature value for a direction s which makes an angle δ from the x-axis, and using the following equation

$$\frac{\partial^2 w}{\partial x \partial y} = \csc 2\delta\left(\frac{\partial^2 w}{\partial s^2} - \frac{\partial^2 w}{\partial x^2}\cos^2\delta - \frac{\partial^2 w}{\partial y^2}\sin^2\delta\right). \tag{16}$$

Alternatively one may choose to use curvature fringe patterns along any three nonparallel directions and use them for the calculation of principal curvatures.

EXPERIMENTAL VERIFICATIONS

In the experiments performed the field lens used had a diameter of 12.7 cm and a focal length of 61 cm. A low power He–Ne laser was used as light course. (Since there is no coherence requirement of the light beam a thermal source with monochromatic filter could also be used.) The magnification was chosen to be one-to-one (i.e. $a = b = 2$). The angle α_x was arranged to be zero so that the field equations (3) and (15) are reduced to, respectively

$$\frac{\partial w}{\partial x} = \frac{Np}{2f} \tag{17}$$

and

$$\frac{\partial^2 w}{\partial x^2} = \frac{N' p^2}{2\lambda f^2}. \tag{18}$$

In all the experiments the models were made of Plexiglas whose surfaces were flat enough to be considered "mirrorlike". The back surface of the model was blackened with paint. Two examples are presented for the slope contouring method: a cantilever beam (6.3 mm × 6.3 mm × 7.6 cm) under endload and a clamped circular plate (dia = 7.6 cm, thickness = 2 mm) under centrally applied concentrated load. The grating used for the experiments had a density of 3.94 lpcm. The resulting fringe patterns and the comparison between experiment and theory of the two examples are shown in Figs. 3 and 4, respectively. The degree of agreement is quite good in both cases.

The same two problems were also used for the demonstration of the curvature contouring method. The experimental procedure was identical to that of slope contouring experiments except that finer gratings were substituted (3.4 lpmm for the cantilever beam and 2 lpmm for the circular plate). The superposition of multiple images of the slope shadowgram created the Moiré enveloping fringes of curvature. The patterns are shown in Figs. 5 and 6, respectively, together with the comparison between experiment and theory. While the curvature fringes of the circular plate are quite distinct, they are a bit hazy in the case of cantilever beam. This is mainly due to the intrinsic property of Moiré fringes that the visibility of rotational mismatch fringes is always better than that of linear mismatch ones except when the element gratings are so fine that the individual lines are not resolved [30]. The degree of agreement between theory and experiment is reasonable but not as good as that in the slope contouring method. This is attributed to the approximation used in deriving eqn (15) and the uncertainty involved in locating the center of curvature fringes.

Since the problem of cantilever beam is one dimensional and circular plate axially symmetric, only one pattern of either slope fringes or curvature fringes is sufficient to yield the stress information completely. In general, however, at least two patterns are needed. As an example the slope and curvature contours along both the x and y directions of a clamped triangular plate under uniform pressure were obtained and are shown in Fig. 7.

APPLICATION TO FLEXUAL WAVE PROPAGATION

The proposed method can also be used for mapping propagating slope and curvature fringes. For nonrepeatable events a high speed camera is necessary. One could either use the optical arrangement of Fig. 1 as is and obtain the propagating slope or curvature fringes along one direction; from which the deflection surface can be obtained by integration and stress information can then be derived from the deflection data. Or, one could modify the optical arrangement by inserting beam splitters after the field lens and using different gratings to generate slope or curvature fringes along different directions. For repeatable events one can obtain all the necessary information sequentially. For this a pulsed light source is necessary, whose pulse duration is short enough to "freeze" the event at different instances. A ruby pulsed laser is an ideal source for such a purpose because its pulse duration is in the nanosecond range. As a demonstration, the method was applied to a cantilever plate (7.6 cm × 7.6 cm × 2 mm) under impact by a swinging ball from a height of 25.4 cm. A ruby laser with pulse

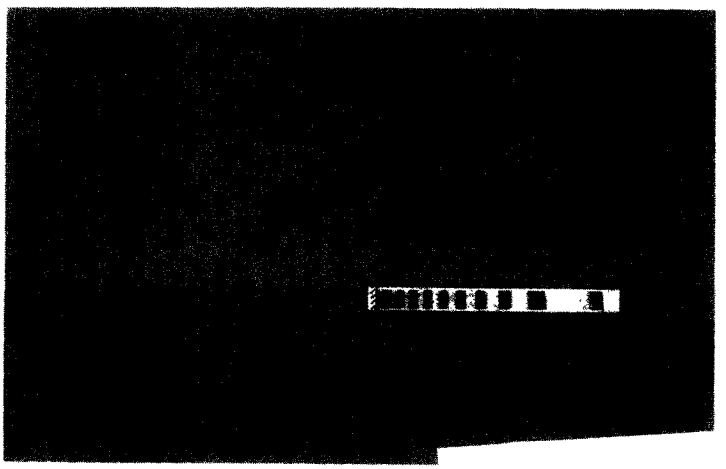

Fig. 3. Slope contours of a cantilever beam under tip load and comparison between theory and experiment.

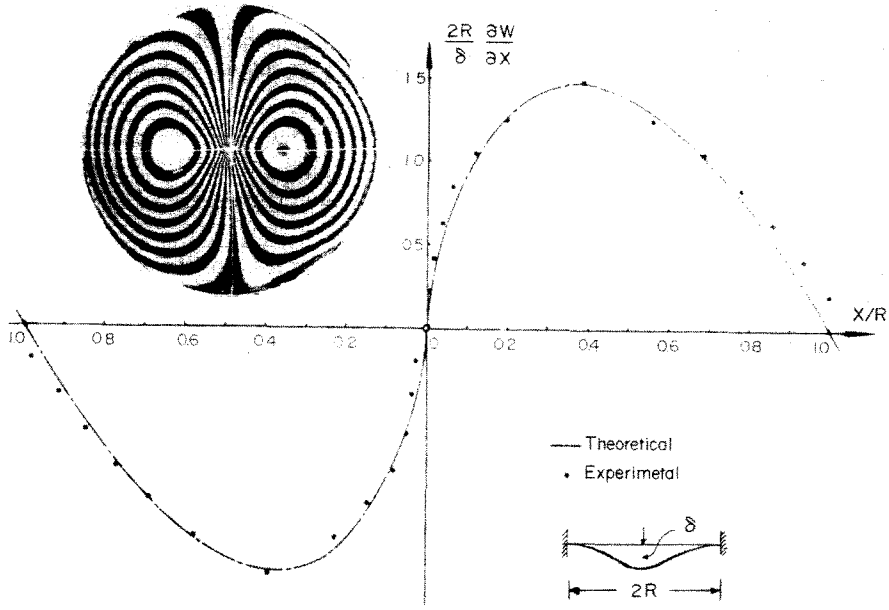

Fig. 4. Slope contours of a clamped circular plate under centrally applied concentrated load and comparison between theory and experiment.

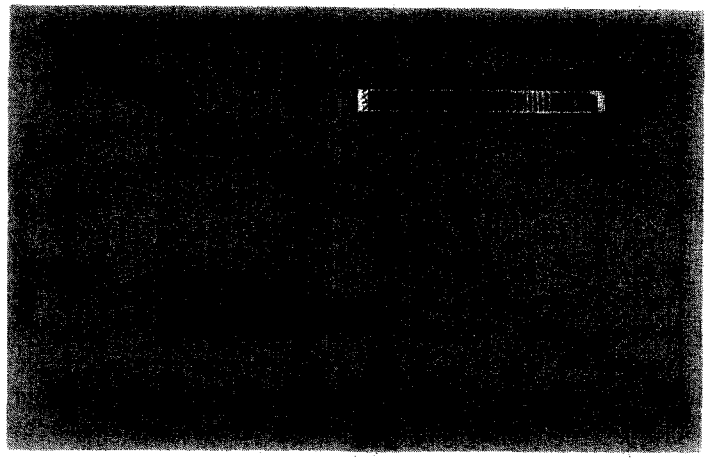

Fig. 5. Curvature contours of a cantilever beam under tip load and comparison between theory and experiment.

duration of 60 nsec was used as the light source and the pictures of propagating slopes (shown in Fig. 8) and curvatures (shown in Fig. 9) were taken at different instances (as given in the figures) after the impact. (The impact signal was fed into a time delay system before triggering the laser.) The gratings used were again of 3.94 and 19.69 lpcm, respectively. Since the method measures either the absolute slope or absolute curvature, any initial nonflatness of the model also appear as fringes; and this was why there were broad fringes at the beginning of the event. The effect of these initial fringes can be eliminated by the procedures discussed in the next section.

It is noted that the contrast of curvature fringes in the dynamic case is not as good as that in the static cases (Figs. 6 and 7). This is so because the total plate deflection at various stages of wave propagation is not as large as in the static cases. However, the fringe positions are nevertheless discernable if one recognizes the fact that they are essentially the loci of points of intersection of shifted slope fringes. Fringe contrast can be improved if a finer grating is used (so that there will be more slope fringes available for interference). This would, of course, result in more initial slope fringes due to plate imperfections.

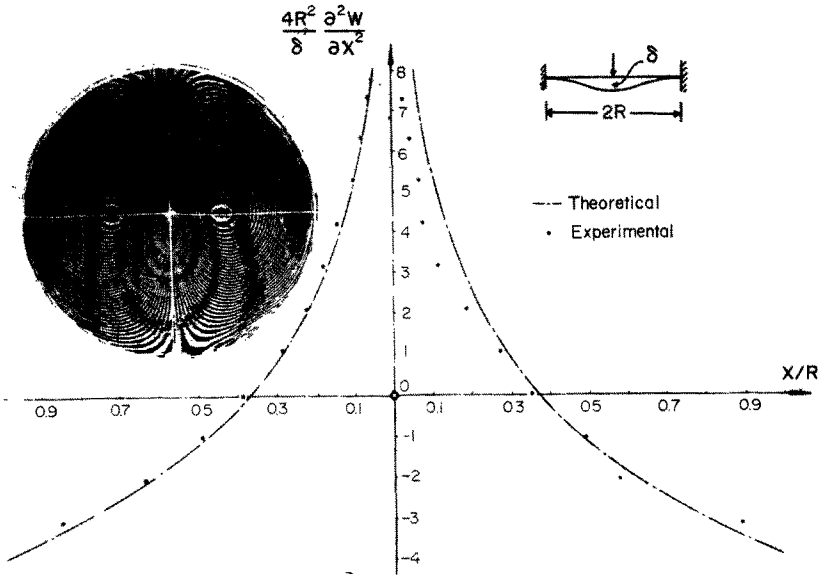

Fig. 6. Curvature contours of a clamped circular plate under centrally applied concentrated load and comparison between theory and experiment.

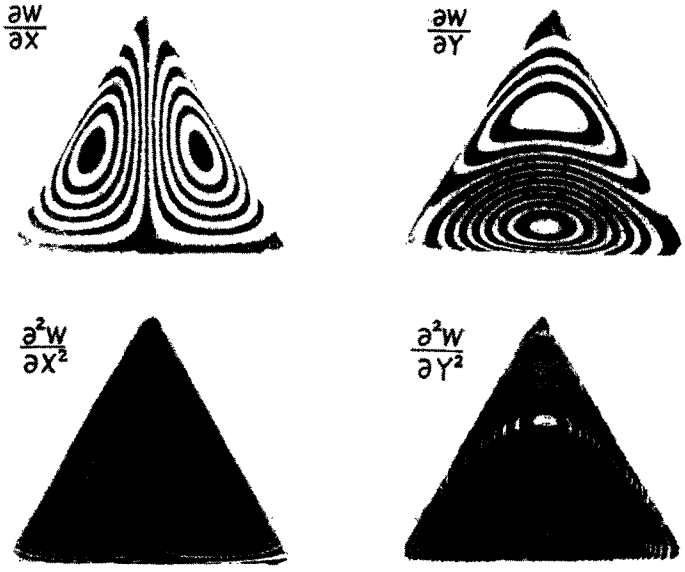

Fig. 7. Slope and curvature contours along x and y directions of a clamped triangular plate under uniform pressure.

DISCUSSION AND CONCLUSION

A simple method is proposed for generating slope and curvature contours of plates under transverse bending. The only equipment needed are a pair of lenses, a monochromatic light source and a few coarse gratings. The method requires that the model surface be specularly reflective. This, however, is not really a serious restriction because of the fact that the natural finishing of common materials such as Plexiglas is usually good enough. For more precise applications one should, of course, polish the model surface. Or one could eliminate the initial fringes due to the nonflatness of the plate by subtracting them from the final ones, either through numerical calculation or through double exposure. For the latter approach it is necessary to introduce a mismatch fringe pattern first[28].

For a given α_x the sensitivity of the method is directly proportional to p/f for slope fringes and $(p/f)^2$ for curvature fringes. In principle in order to have high sensitivity one would select a lens with long focal length and a grating of fine pitch. However, what comes with fine gratings is

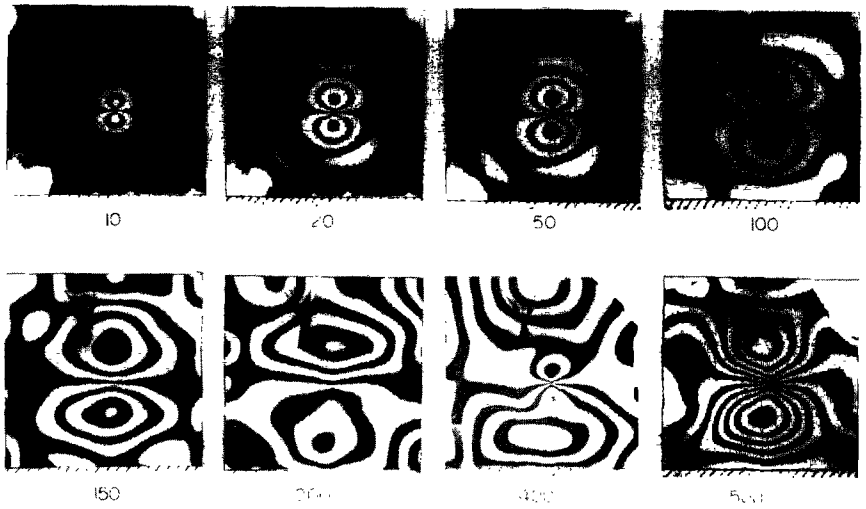

Fig. 8. Propagating slope contours of a square cantilever beam under impact (numbers in μsec).

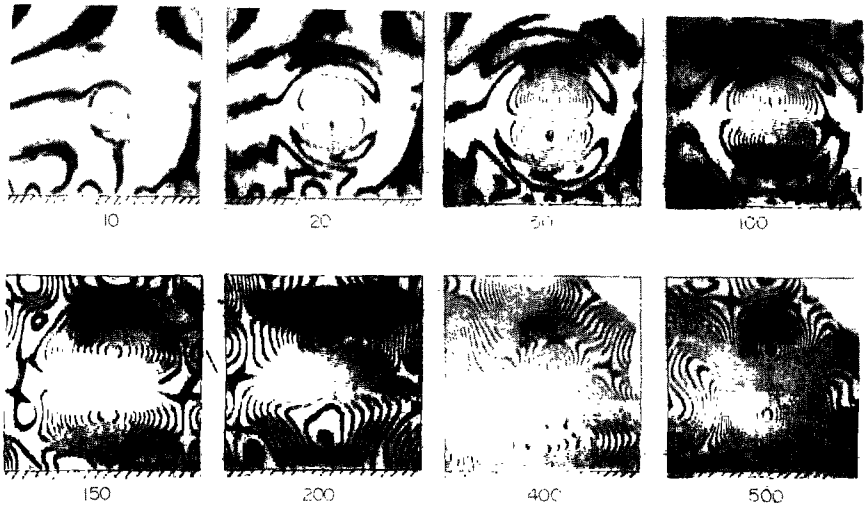

Fig. 9. Propagating curvature contours of square cantilever beam under impact (numbers in μsec).

the diffraction effect which generates shifted multiple images. Thus a happy medium has to be reached depending upon what is considered to be the tolerable shift of images. For slope contouring it is the maximum shift at which no overlapping fringes are present; and for curvature contouring it is the maximum shift that the error due to finite difference approximation is acceptable. It can be shown that for a field lens of 61 cm focal length the usable range of grating line density is about 4–8 lpcm for slope contouring and 20–40 lpcm for curvature contouring. The corresponding sensitivities are then on the order of 10^{-3} rad and 10^{-3} cm^{-1}, respectively.

The sensitivity of the method for slope determination compares favorably with that of the original Ligtenberg method[13], and is of the same order of magnitude as that of the later versions[16, 17]. However, these later versions usually employ gratings with line density one order of magnitude higher and requires optical spatial filtering to render the fringes visible. The proposed method is better than the Ligtenberg method in yet another aspect: its usage of light energy is more economical rendering it more susceptible to high speed photography. The fact that the method yields high sensitivity fringes directly without double exposure (as does the Ligtenberg method) is perhaps its best asset. Of course the need of a field lens is also the method's limitation in that one cannot employ large size models. Furthermore lens aberration also contributes to its error if double exposure is not used.

Another source of error is the approximation used [i.e. $\beta \sim \alpha_x$ in deriving eqn (15)]. For a

lens of 12.7 cm in diameter and 61 cm in focal length, it can be shown that the maximum error in fringe order for a 7.63 cm (3 in.) model is 4.2%.

The method also compares favorably with other slope contouring techniques. For example, the Salet–Ikeda method[18] employs a more complicated optical system in which a geometric target has to be projected onto a mirror-surface model and then received via a pinhole viewing system. The Moiré methods of Theocaris[19, 20] usually result in relatively inferior fringes because of the very nature of Moiré phenomenon. The method is complimentary to the laser speckle methods of Hung[21], and Chiang and Jung[22] in that it can only be applied to mirror-surface models whereas the speckle methods only to matte surface models.

The method's capability of real time contouring curvature in a full-field manner is an unique feature as compared to other methods where either superposition or double exposure[23–25], or a two-step procedure[26] is needed.

It should be noted that while the method is devised mainly for the purpose of experimentally solving plate bending problems, it can be applied to other metrological problems as well.

Acknowledgements—We would like to thank the National Science Foundation for supporting the work reported in this paper. The paper was presented at the 1974 DGaO-CbO meeting in Belgium[28] and a similar work from a different viewpoint was independently proposed by Assa[30]. We thank Mrs. P. Wolosin for typing the manuscript.

REFERENCES

1. J. N. Goodier and C. H. Lee, An extension of the photoelastic method of stress measurement to plates in transverse bending. *J. Appl. Mech., Trans. ASME* **63**, A27–9 (1941).
2. D. C. Drucker, The photoelastic analysis of transverse bending of plates in the standard transmission polariscopes. *J. Appl. Mech., Trans. ASME* **64**, A161–164 (1942).
3. P. S. Theocaris, Moiré Methods in Plates. *Proc. Int. Assoc. Shell Struct.* (*Symp.*), pp. 913–989, Warsaw. North Holland, Amsterdam (1963).
4. L. Pirodda, Principie applicazioni di un metodo fotogrammetrico basato sullimpiego del Moiré. *Revista di Ingegneria* **12**, 913–947 (April 1969).
5. B. C. Dykes, Analysis of displacements in large plates by the grid-shadow moiré technique. In *Exp. Str. Analysis and Its Influence on Design* (Edited by M. L. Meyer), pp. 125–134. Cambridge University Press (1971).
6. H. Takasaki, Moiré topology. *Appl. Optics* **9**, 1457–1472 (June 1970).
7. F. P. Chiang, A shadow-Moiré method with two discrete sensitivities. *Exp. Mech. Proc. SESA* **15**(10), 382–385 (1975).
8. F. P. Chiang and B. Ranganayakamma, Deflection measurement using Moiré gap effect. *Exp. Mech.* **11**(7), 296–302 (1971).
9. R. E. Rowlands and I. M. Daniel, Application of holography to anisotropic composite plates. *Exp. Mech. Proc. SESA* **12**(2), 75–82 (Feb. 1972).
10. J. Der Hovanesian and Y. Y. Hung, Moiré contour-sum and contour-difference and vibration analysis of arbitrary objects. *Appl. Optics* **10**(12), 2730–2738 (1971).
11. J. Der Hovanesian, R. E. Haskell and R. L. Powell, Use of a projected-ruling Moiré method for vibration and deflection measurement of three-dimensional structures. *Proc. Engng Application of Holography* (*Symp.*) (16–17 February 1972).
12. R. P. Khetan and F. P. Chiang, A general analysis of projection Moiré methods. Developments in Mechanics, Vol. 8, *Proc. 15th Midwestern Mech. Conf.*, Univ. of Illinois (Chicago Circle) (22–26 March 1977).
13. F. K. Ligtenberg, The Moiré method: A new experimental method for the determination of moments in small slab moments. *Proc. SESA* **12**(2), 83–98 (1954).
14. G. Rieder and R. Ritter, Krummungsmessung an belasleten platem nach dem Ligtenbergschen Moiré-verfahren. *Forschung im Ingenieur Wesen* **31**(2), 33–44 (1965).
15. F. P. Chiang and J. Treiber, A note on Ligtenberg's reflective Moiré method. *Exp. Mech.* **10**(2), 537–538 (1970).
16. F. P. Chiang and G. Jaisingh, Dynamic Moiré methods for the bending of plates. *Exp. Mech.* **13**(4), 168–171 (1973).
17. F. P. Chiang and G. Jaisingh, A new optical system for Moiré methods. *Exp. Mech.* **14**(11), 459–462 (1974).
18. J. P. Duncan and C. J. E. Brown, Slope contours in flexed elastic plates by Salet–Ikeda technique, *Proc. 1st Int. Cong. Exp. Mech.* (Edited by B. G. Rossi). SESA (1963).
19. P. S. Theocaris, Moiré patterns of slope contours in flexed plates. *Exp. Mech.* **6**(4), 212–217 (1966).
20. P. S. Theocaris, Slope measurement by means of Moiré fringes. *J. Sci. Instruments* **42**, 607–610 (1965).
21. Y. Y. Hung, Measurement of slopes of structural deflections by speckle-shearing interferometry. *Exp. Mech. Proc. SESA* **14**(7), 281–285 (1974).
22. F. P. Chiang and R. M. Juang, A method of laser speckle interferometry for plate bending problems. *Appl. Optics* **15**(9), 2199–2204 (Sept. 1976).
23. J. P. Duncan and P. G. Sabin, An experimental method for recording curvature contours in flexed elastic plates. *Exp. Mech. Proc. SESA* **15**(1), 22–28 (1965).
24. H. Saito, I. Yamaguchi and K. Hachinine, An application of holographic interferometry to stress analysis of elastic bending of plate. *Scientific Papers of Inst. of Physics and Chemistry Res.* **64**(4), 101–111 (1970).
25. V. Heise, A Moiré method for measuring plate curvature. *Exp. Mech. Proc. SESA* **7**(1), 47–48 (1967).
26. F. P. Chiang and M. Bailangadi, A method for direct determination of small curvatures. *J. Appl. Mech., Trans. ASME* **42**(1), 29–31 (1975).
27. V. Ronchi, Forty years of history of a grating interferometer. *Appl. Optics* **3**(4), 437–451 (1964).
28. F. P. Chiang and T. Y. Kao, An optical method for generating slope and curvature contours of bent plates. (Summary)

Proc. Joint Meeting of German Optical Society (DGaO) *and Belgium Optical Committee* (CbO), Brugge, Belgium, p. 58 (4–8 June 1974).
29. A. Assa, Some New Optical Methods for Use in Experimental Stress Analysis. Ph.D. Thesis Israel Institute of Technology (July 1975).
30. F. P. Chiang, A method to increase the accuracy of Moiré method. *J. Engng Mech. Div., Proc. ASCE* **91(EM1)**, 137–149 (Feb. 1965).
31. F. P. Chiang and T. Y. Kao, An Optical Method of Generating Slope and Curvature Contours of Bent Plates. Rep. No. 313, College of Engineering and Applied Science, State University of New York at Stony Brook (Feb. 1978).